Optimized Production Assessment, Compartmental Modeling and Dosimetric Evaluation of ^{177}Lu- PSMA-617 for Clinical Trials

Mehdi Sharifi[1], Hassan Yousefnia[1], Ali Bahrami-Samani[1], Amir Reza Jalilian[1], Samaneh Zolghadri[1,*], Mahdokht Vaez-Tehrani[2] and Stephan Maus[3]

[1]*Nuclear Science and Technology Research Institute (NSTRI), Tehran, Iran, Postal code: 14155-1339*

[2]*Energy Engineering and Department of Physics, Amir Kabir University of Technology, Tehran, Iran*

[3]*Clinic of Nuclear Medicine, University Medical Centre Mainz, Langenbeckstrasse 1, D-55131 Mainz, Germany*

Abstract: ^{177}Lu-PSMA-617 was prepared at the optimized conditions (95°C, 15-18 µg peptide, 35-40 min; solid phase purification) using ^{177}Lu obtained from ^{176}Lu(n, γ)^{177}Lu reaction(>98%, ITLC, HPLC, S.A. 22-24 TBq/mM) followed by stability (up to 48 h), biodistribution studies (up to 168 h), planar imaging, compartmental modeling and dosimetry estimations via Sparks's extrapolation method in human organs. Kidney is the critical organ with the dose of 0.067 mGy/MBq and the radiopharmaceutical can be safely used in trials considering the human dose.

Keywords: Biodistribution, Lu-177, PSMA-617, SPECT imaging, Compartmental modeling.

INTRODUCTION

Prostate cancer (PC) known as the second most popular cancer in men [1], can be treated if detected in the early stages. While the prostate specific membrane antigen (PSMA) expression increased significantly in prostate cancer tissue [2], it has been characterized as a viable and useful biomarker over the twenty years from its discovery and many radiolabeeled compounds of PSMA have been developed for the diagnosis and therapy of PCs [3, 4].

PSMA-HBED-CC labelled with ^{68}Ga represents a successful novel PSMA inhibitor radiotracer and has recently demonstrated its suitability in individual first-in-man studies [5], the HBED-CC chelator (N,N′-bis[2-hydroxy-5-(carboxyethyl)benzyl] ethylenediamine-N,N′-diacetic acid)is not suitable for radiolabeling with therapeutic radiometals [6]. Beside the slightly modified chemical structure of the molecules synthesized for binding to PSMA, these molecules differ mainly in the selection of the chelator for the complexation of the desired radionuclide [7-9].

1,4,7,10-tetraazacyclododecane-1,4,7,10-tetraacetic acid, known as DOTA, and its analogues are the mostly used chelator for the complexation of radiometals specially to small molecules [10, 11] and form stable complexes with a broad range of radiometals especially with ^{90}Y and ^{177}Lu.

Recently, 2-[3-(1-Carboxy-5-{3-naphthalen-2-yl-2-[(4-{[2-(4,7,10-tris-carboxymethyl-1,4,7,10-tetraaza-cyclododec-1-yl)-acetylamino]-methyl}-cyclohexanecarbonyl)-amino]-propionylamino}-pentyl)-ureido]-pentanedioic acid (PSMA-617) has been introduced as the DOTA-based synthesized PSMA (Figure **1**) [12]. ^{131}I-labeled PSMA ligand (^{131}I-MIP-1095) indicated promising results as a new tumour targeting agent [13]. However, some limitations of ^{131}I such as high radiation burden and even hampering in most countries make ^{177}Lu as a better candidate than ^{131}I. ^{177}Lu with favourable physical characteristics [$t_{1/2}$=6.73 d, $E_{\beta max}$ = 497 MeV, Eγ=112 keV (6.4%), 208 keV (11%)], has been identified as one of the most promising radionuclides for the therapeutic applications [14].

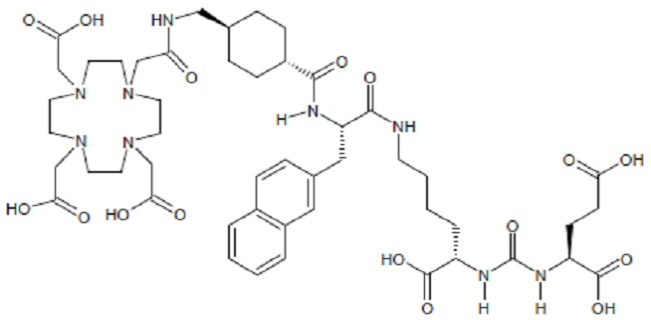

Figure 1: Chemical structure of PSMA-617.

^{177}Lu labeled PSMA-617 has newly been introduced, showing high potential in the clinical management of advanced PCs in its first human study [15]. Despite of the excellent characteristics of ^{177}Lu-PSMA-617 as the novel theranostic drug in the

*Address correspondence to this author at the Material and Nuclear Fuel Research School, Nuclear Science and Technology Research Institute (NSTRI), Tehran, Iran, Postal code: 14155-1339; Tel: +982188221103; Fax: +982188221105; E-mail: szolghadri@aeoi.org.ir

E-ISSN: 2408-9788/17

treatment of the advanced PC, there is no adequate published data in preclinical aspects of this radiopharmaceutical and therefore more preclinical data on its biodistribution and its absorbed dose in different organs is required for its performance evaluation.

Absorbed dose is an important parameter in evaluating the hazards regarding the administration of radiopharmaceuticals and so the maximum amount of activity that should be assumed. This concern is naturally increased in therapeutic approach where a significant absorbed dose may be received by other organs and in particular by radiosensitive organs [16]. At the present time, in nuclear medicine, the radiation absorbed dose assessment resource (RADAR) is identified as the mostly used method for the internal dose calculation [17].

Evaluation of the radiation absorbed dose from biodistribution data in animals is a necessary requirement for the clinical use of a new radiopharmaceutical [18]. Several approaches have been previously offered to estimate the human organs uptakes using the animal data including dose by factor, similar drug, pharmacokinetic ally guided, and comparative approaches and also the methods presented by Sparks *et al*. [19, 20]. Sparks *et al*. hasexplained four extrapolation methodestothis action [21]: 1. no extrapolation, 2. relative organmass extra-polation, 3. physiological time scaling 4. mass and time scalings.

Compartmental modeling, as the most commonly used method for describing the uptake, metabolism and elimination of radioactive tracers in tissue [22-24], can specify that all molecules of tracer delivered to the system (*i.e*., injected) will at any given time exist in one of many compartments [25]. The most common use of compartmental modeling is the mathematical description of the distribution of a radiolabeled complex throughout the body [22, 26]. The compartmental model also describes all of the possible transformations that can occur to the complex, permitting it to shift from one compartment to the other compartment and so on. So, the fractional rate of this change of the complex concentration in one compartment is called a rate constant, generally identified as "*k*" with units of inverse time [25]. Therefore, the biological modeling by Compartmental analysis can solve the abovementioned requirements restrictions in extrapolation methods.

In this research work, the authors attempted to introduce the supplementary preclinical data of ^{177}Lu-PSMA-617 and related aspects of its production. The optimized conditions for the preparation of this new therapeutic complex was investigated while the radiochemical purity was assessed using both of HPLC and ITLC procedures. Also, with the aim of assessing the uptake of the complex in normal tissues, the biodistribution of the radiolabeled agent was investigated in healthy rats at specified time intervals after injection by sacrifice and SPECT imaging. Finally, dosimetry estimations in human organs were performed via relative organ mass extrapolation method using biodistribution Compartmental modeling data. The obtained human absorbed dose were comparable with the human dosimetry data reported in the other literature.

EXPERIMENTAL

^{177}Lu was produced by neutron bombardment of ^{176}Lu via ^{176}Lu (n,γ)^{177}Lu nuclear reaction. Enriched Lu_2O_3 (^{176}Lu, 52%)was obtained from ISOTEC Inc. PSMA-617 was supplied from ABX (Radeberg, Germany). All of the other chemical reagents and Whatman No. 2 paper were purchased from Sigma-Aldrich Chemical Co and (Heidelberg, Germany). Whatman (Buckinghamshire, U.K.), respectively. Radio-chromatography of the papers was performed by a thin layer chromatography scanner (Bioscan AR2000, Paris, France). The activity of the samples was measured by a p-type coaxial high purity germanium (HPGe) detector (model: EGPC 80-200R) coupled with a multichannel analyzer system (GC1020-7500SL, Canberra, U.S.A.). Reverse phase high performance liquid chromatography (RP-HPLC) was performed for radiolabeling and specific activity analyzed of the final product using a KNAUER-D-14163 system, Berlin, Germany. Planar images were captured by a dual head SPECT system (DST-XL, SMV, Buc, France). All values were expressed as mean ± standard deviation (Mean ± SD) and the data were compared using Student's T-test. Statistical significance was defined as $P<0.05$. The United Kingdom Biological Council's Guidelines on the Use of Living Animals in Scientific Investigations, second edition was considered as the basis of animal studies.

Production and Quality Control of $^{177}LuCl_3$ Solution

100 µg of enriched Lu_2O_3 (^{176}Lu, 52% from ISOTEC Inc.) was irradiated in a research reactor at a thermal neutron flux of 5×10^{13} n.cm^{-2}·s^{-1} for 5 d. Then, the irradiated target was dissolved in 200 µL of 1.0 M HCl and diluted to the appropriate volume with ultra pure

water, according to the method described in the previous related studies [27]. Beta spectroscopy as well as HPGe spectroscopy was utilized for the assessment of radionuclidic purity. Instant thin layer chromatography method (ITLC) was used for checking the radiochemical purity, while, 10 mM DTPA (pH = 4) and ammonium acetate 10%: methanol (1:1) were considered as the solvent systems.

Radiolabelling of PSMA-617 with $^{177}LuCl_3$

As proposed in previous investigation by authers [12], a stock solution of PSMA-617 in the distilled water was added to the vial containing $^{177}LuCl_3$, while, several experiments were performed for the determination of the optimized conditions. Ultimately, the final solution was passed through a C_{18} Sep-Pak column preconditioned with 5 mL ethanol, 10 mL water and 10 mL air, respectively. The column was then washed with 1 mL ethanol and 9 mL of 0.9% NaCl.

Both HPLC and ITLC methods were applied for the radiochemical purity assessment. HPLC was carried out by means of MZ-Analysentechnik, ODS-H 5µm (100×4.0 mm) column. The following mobile phases were employed: A= Ultra pure water-TFA 1% (V/V); B=Acetonitrile HPLC Grade using gradient-elution: 0-3 min, A:100%, B: 0%; 3-10 min, A:50%, B: 50%; 10-15 min, A:0%, B:100%; Flow rate:1.5 mL/min, Injection volume: 20 µL. In the case of ITLC, 0.9 % NaCl and 0.1 M sodium citrate were selected as the mobile phases.

STABILITY TESTS

This step of the current study was performed in accordance with some of the previous same works [28]. A given amount of complex (approximately, 200 µCi) was kept at room temperature for 48 h while being checked by ITLC at specified time intervals (2, 4, 24, 48 and 72 h). Also, for serum stability test, 200 µCi of ^{177}Lu-PSMA-617was subjoined to 300 µL offreshlyhuman serum and then the mixture was incubated at 37°C for 48 h, where as its radiochemical purity was analyzed by ITLC method at 2,4, 24, 48 and 72 h after preparation.

Biodistribution of the Radiolabelled Complex in Rats

The final radiolabelled complex was injected intravenously into the rats (100 µL, 5.55 MBq). The animals were sacrificed at given times after injection (2, 4, 24, 48, 72 and 168 h) using the animal care protocols. Blood samples were quickly taken from the rats. The weight and activity of each tissue was measured using a calibrated blance and a p-type coaxial HPGe detector coupled with a multi-channel analyser and according to the relationships used to calculation of the activity concentration [29]. Five rats were sacrificed for each interval. Finally, the percentage of injected dose per gram (%ID/g) for different organs was computed according to the previous literatures [30].

HUMAN ABSORBED DOSE ASSESSMENT

Calculation of Accumulated Activity Using Compartmental Modeling

Calculation of accumulated activity is the first step in human absorbed dose assessment. The accumulated source activity for each animal organ was calculated via plot of the non-decay corrected %ID/g- time curve and according to Equation 1:

$$\tilde{A} = \int_{t_1}^{\infty} A(t)\, dt \qquad (1)$$

where $A(t)$ is the activity of each organ at time t.

Cumulative activity in organs of interest can be determined by numeric or compartmental models [31]. In fact, the accumulated activity for each source organ was calculated by substituting the formulas obtained from the compartmental modeling in Equation 3.

Compartmental analysis support the radiopharmaceuticals design permitting a mathematical separation of tissues and organs to determinate the concentration of activity in each fraction of interest and pointing toward inconsistency in biodistribution and dosimetry studies. Additionally, by compartmental analysis it is possible to consider different chemical species and to predict metabolites [32]. In this model each compartment defines one possible state of the tracer, specifically its physical location (for example, intravascular space, extracellular space, intracellular space, and synapse) and its chemical state (*i.e.*, its current metabolic form or its binding state to different tissue elements, such as plasma proteins, receptors, etc.) [25].

Extrapolation of Animal Data to Human Ones

The next step to estimate the human absorbed dose is to extrapolate the animal accumulated activity to

human ones. Preclinical animal studies are used to develop the new radiopharmaceuticals with the goal of determining a preliminary approximation of absorbed dose in human organs. In the previous attempts, in direction to estimate the absorbed dose of human organs using animal data, several extrapolation techniques have been applied to compensate the differences of metabolism, anatomy and biodistribution of radiopharmaceuticals between animals and humans.

The accumulated activity of human organs was then calculated using relative organ mass extrapolation (Equ. 4) [19].

$$\tilde{A}_{Human\ organ} = \tilde{A}_{Animal\ organ} \times \frac{Organ\ mass_{human}/Body\ mass_{human}}{Organ\ mass_{animal}/Body\ mass_{animal}} \quad (4)$$

Equivalent Absorbed Dose Calculation

Calculation of the absorbed dose in human organs was accomplished by means of RADAR formalism as described in previous studies [27]:

$$D = \tilde{A} \times DF \quad (5)$$

where $\tilde{A}$ is the accumulated activity for each human organ, and DF expressed in mGy/MBq.s is a factor considering the physical decay characteristics of the radionuclide, the range of the emitted radiations, and the organ size and configuration [33]. In this research, DFs have been taken from the amount presented in OLINDA/EXM software [34].

Effective Absorbed Dose Calculation

The effective absorbed dose for each organ was calculated by multiplying the tissue weighting factor (W_T) and the equivalent absorbed dose (H_T) by means of the following Equation

$$E = \sum_T W_T H_T \quad (7)$$

W_T was obtained from the reported value in ICRP 103.

Imaging Studies

Planar images were obtained after 24 and 48 hours of intravenous administration of the radiolabelled complex in the healthy Syrian rats by a dual head SPECT system, whereas the mouse-to-high energy septa distance and the useful field of view (UFOV) were considered equal to 12 cm and 540 mm×400 mm, respectively.

RESULTS AND DISCUSSION

The specific activity of 90-100 GBq/mg was obtained for ^{177}Luin this research. A p-type coaxial HPGe detector was used to check the radionuclidic purity. Whereas the peaks of 112 and 208 keV related to ^{177}Lu were observed, the radionuclidic purity was obtained more than 99.9 %. Only a few impurity was obtained which related to ^{177m}Lu. Radiochemical purity of the $^{177}LuCl_3$ solution was checked using Whatman No.2 paper and in solvent systems of 10 mM DTPA and 10% ammonium acetate:methanol (1:1). In a mixture of 10 mM DTPA solution (pH 5), free $^{177}Lu^{3+}$ cation is converted to more lipophilic ^{177}Lu-DTPA form and migrates to higher R_f (R_f.0.8). In the case of 10% ammonium acetate:methanol (1:1), $^{177}Lu^{3+}$ remains at the origin while other ionic species would migrate to higher R_fs. The results indicated the radiochemical purity of higher than 98%.

Changing in different reaction parameters such as the ligand concentration, pH, temperature and reaction time was used to obtain the maximum complexation yields. The effect of pH on complexation yield was studied by varying the pH of the reaction mixture using HEPES from 3 to 5. The results indicated that the optimum pH for radiolabeling is 4-4.5. Also, the effect of the ligand amount on the radiochemical yield was checked. The results indicated that by adding the certain amount of the ligand (15 µg, 14.4 nmol) to the vial containing $^{177}LuCl_3$ (with a maximum activity of 10 mCi), ^{177}Lu-PSMA-617 can be prepared with the complexation yield of higher than 99% and specific activity of 22-24 TBq/mM. While the temperature of 90-95 °C is required, the experiments showed that 35-40 min is the optimum radiolabeling reaction time.

Both HPLC and ITLC methods was applied to check radiochemical purity of the radiolabelled complex. In the case of ITLC method, in both 0.1 M sodium citrate and 0.9% NaCl as the mobile phases with Whatman No.2 as the stationary phase, the radiolabelled compound remains at the origin, while free ^{177}Lu cation migrates to higher R_f (Figure **2**).

HPLC analysis showed that the fast eluting compoundwas hydrophilic ^{177}Lu cation (1.0 min), while ^{177}Lu-PSMA-617 with high molecular weight was eluted after 4.47 min (Figure **3**). Both the HPLC and ITLC chromatograms showed the radiochemical purity of more than 99%.

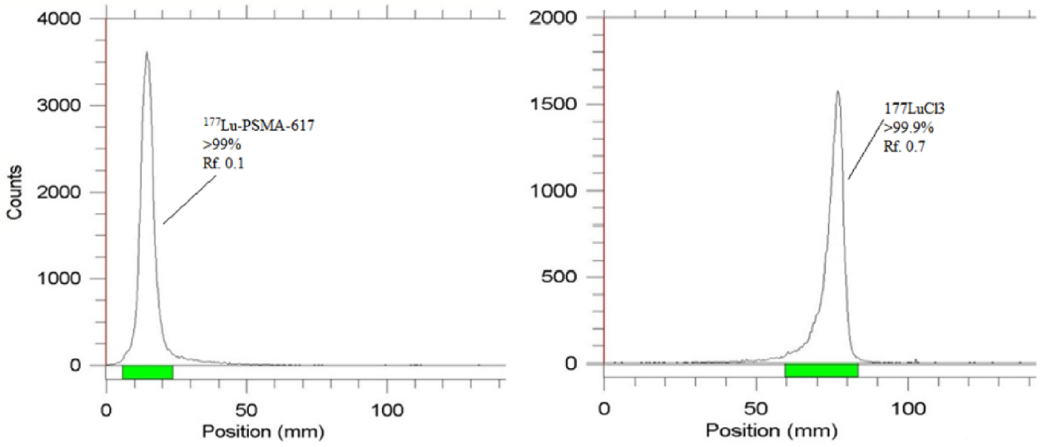

Figure 2: ITLC chromatogram of 177LuCl3 (right) and 177Lu-PSMA-617 (left) in 0.9% NaCl using Whatman No.2.

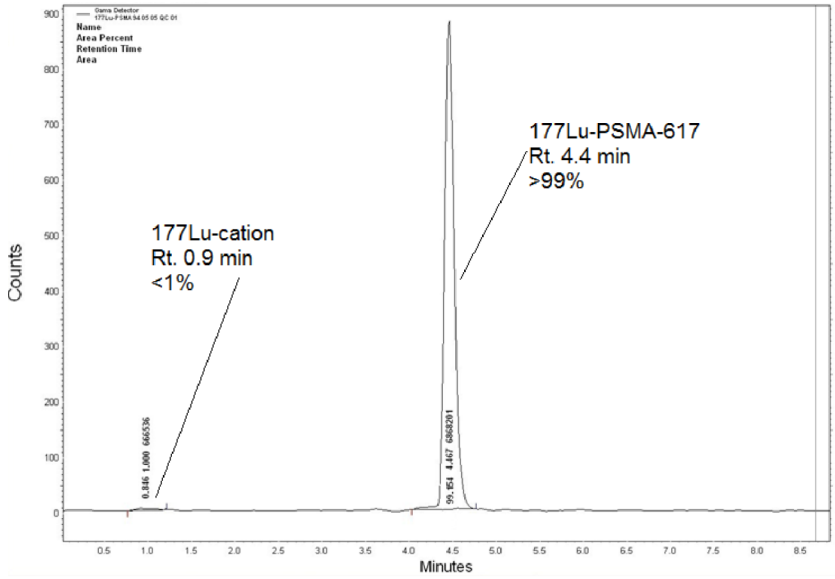

Figure 3: HPLC chromatogram of 177Lu-PSMA-617 prepared at optimized conditions.

The stability of the radiolabelled complex was investigated in room temperature and in human serum at 37 °C. The radiochemical purity of the complex remained >98% at room temperature and in freshly prepared human serum at 37 °C even after 48 h of preparation.

The biodistribution data of ^{177}Lu-PSMA-617was obtained following sacrifice and the activity measurement of each tissue and calculated as the percentage of area under the curve of the related photo peak per gram of tissue (% ID/g). However, in this research, the carrier added ^{177}Lu is used in the experiments, but it seems that the biodistribution of no carrier added and carrier added ^{177}Lu-PSMA be identical in accordance to the other previous research which indicated the same biodistribution for carrier added and no carrier added radiolabeled compound [35].

The results demonstrated significant uptake in the kidneys as the major route of excretion, which is due to the physiological PSMA expression in the kidneys [2] and is in accordance to the other reported radiolabelled complex of PSMA [36]. The maximum uptake in the kidney was occurred at 2 h post injection while decrease rapidly with time (Figure **4**).

Less than 0.2% of the injected dose per gram was observed in blood after 2 h, which shows fast clearance from the circulation and is a major advantage since the dose to non-target organs reduce significantly. While

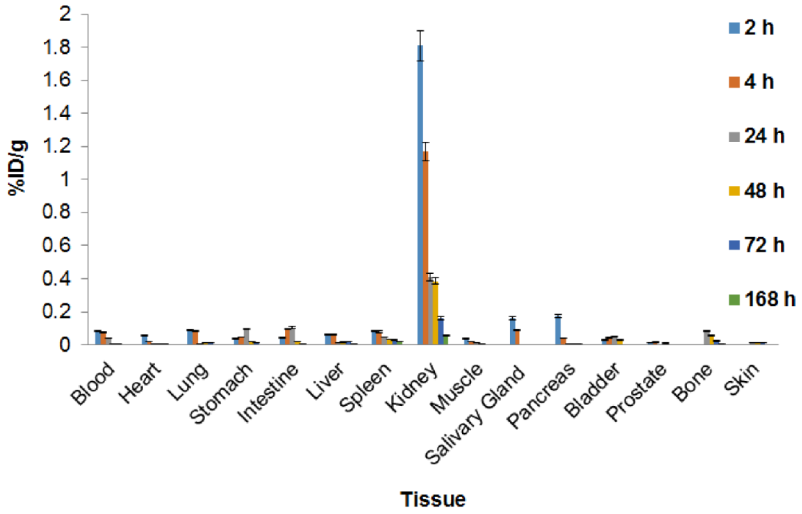

Figure 4: Percentage of injected dose per gram (%ID/g) at 2, 4, 24, 48, 72 and 168 h after intravenously injection of 177Lu-PSMA-617 (5.55 MBq) into breast adenocarcinoma-bearing BALB/c mice (%ID/g: percentage of injected dose per gram of tissue calculated based on the area under curve of 112 keV peak in gamma spectrum) (n=5).

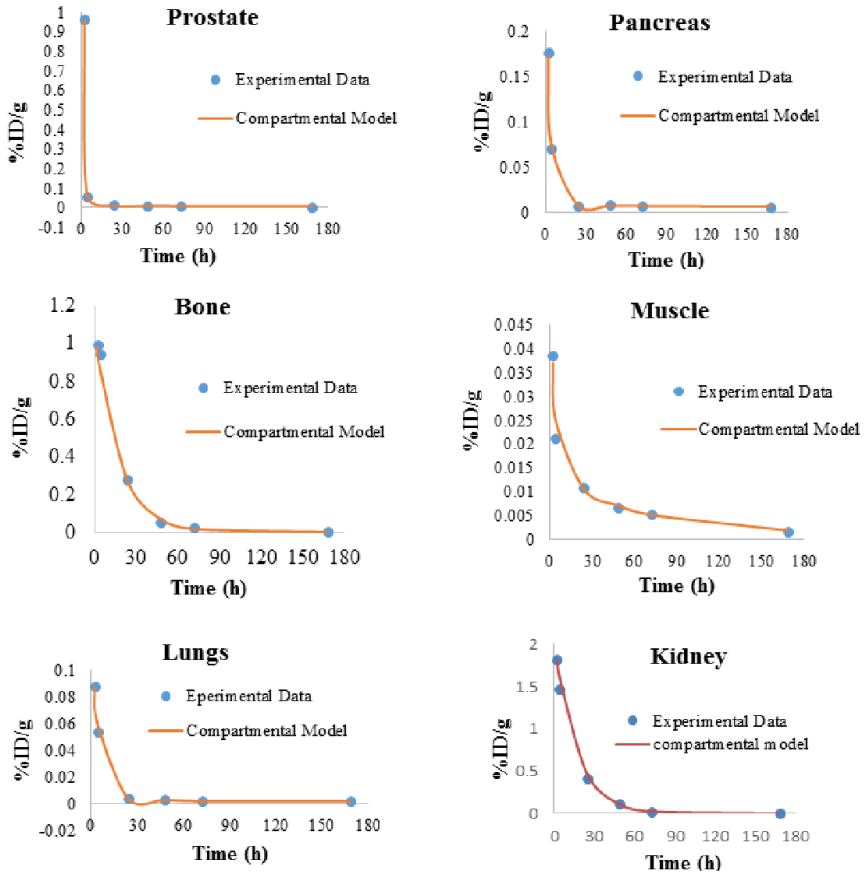

Figure 5: The non-decay corrected injected activity curves after 177Lu-PSMA-617 injection to animal models for prostate, pancreas, bone, muscle, lungs and kidneys.

the accumulation of the activity in the spleen and liver diminish slightly with time, intestine uptake reaches its maximum amount at 24 h post injection.

Recently, a study has been reported on the synthesis of DOTA-conjugated PSMA inhibitor (PSMA-617) and its radiolabeling with $^{67/68}$Ga and ^{177}Lu [3].

However, this study has more emphasized on the synthesis of this new PSMA analogue, the biodistribution of the radiolabelled complexes were also investigated in BALB/c nu/nu mice bearing LNCaP xenografts but in the limited times after injection. In the case of ^{177}Lu-PSMA-617, the biodistribution data only was presented after 1 h and 24 h post injection, while according to the half-life of ^{177}Lu (6.7 d), more preclinical data on healthy rats especially in the longer intervals seems to be essential.

In this study, with regard to the importance of the activity distribution through non-target organs which lead to the undesirable absorbed dose, ^{177}Lu-PSMA was prepared and biodistribution studies were carried out in different organs of the Syrian rats at specified intervals (2 to 168 h) post injection. Consistent with the previously reported literature, significant accumulation was observed in the kidneys with a rapid decrease with time.

Also, as mentioned previously, a small %ID/g was observed in the lung at 2 h post injection which is in great accordance with Benešová *et al*. Findings [4]. Some uptakes of the activity has been observed in the salivary gland. Figures **6** and **7** demonstrate the wash out of activity from each critical issue during experiment time frame.

The accumulated activity for each animal organ was calculated by integration of the formulas obtained from

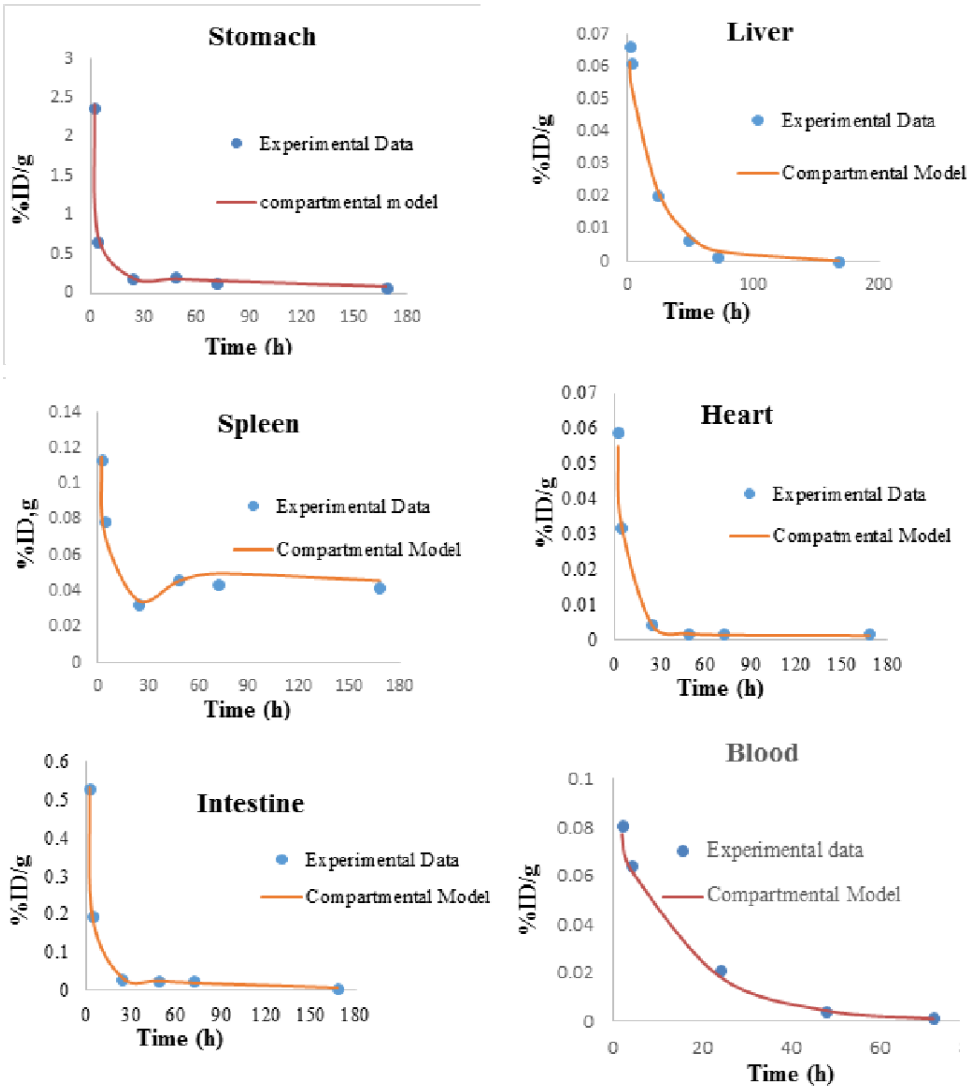

Figure 6: The non-decay corrected injected activity curves after 177Lu-PSMA-617 injection to animal models for stomach, liver, spleen, heart, intestine, and blood.

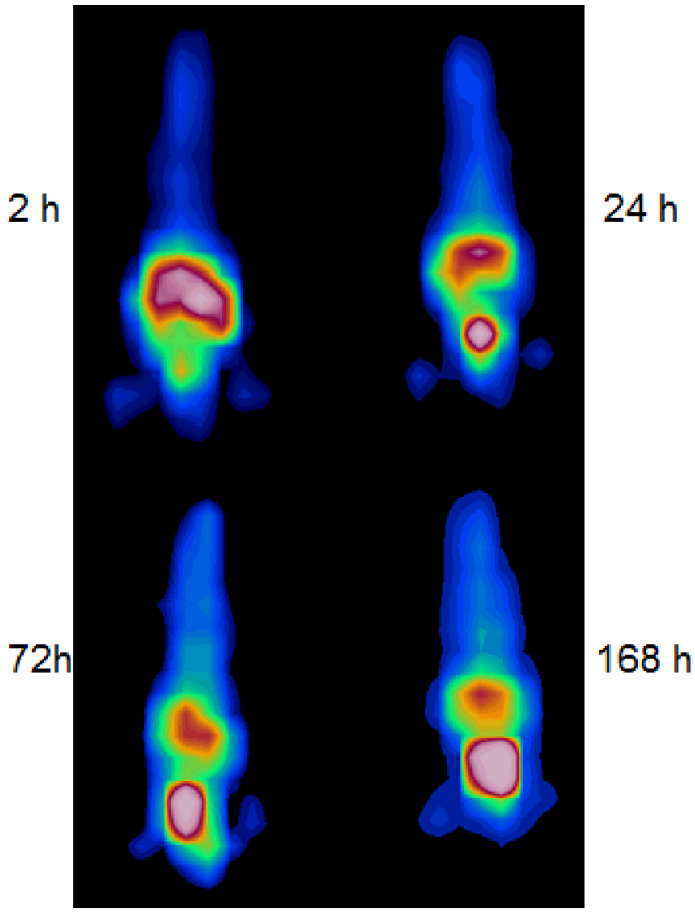

Figure 7: SPECT images of 177Lu-PSMA-617 following 5.55 MBq injections in BALB/c nude mice bearing adenocarcinoma breast tumor after 5 min (**a**) 30 min (**b**) 60 min (**c**).

the compartmental modeling. The non decay corrected injected activity curves, the related formulas and the calculated accumulated activity for each source organ have been shown in Tables **1** and **2**, respectively.

Human absorbed dose estimation was carried out by RADAR method based on biodistribution data in the rat organs. The equivalent and effective absorbed dose in human organs after intravenously injection of ^{177}Lu-PSMA-617 are presented in Table **2**. The highest absorbed dose for ^{177}Lu-PSMA-617 is observed in the kidney with 0.067 mGy/MBq.

SPECT images were acquired at 2, 24, 72 and 168 h after ^{177}Lu-PSMA-617 injection in the normal Syrian rats (Figure **7**). As it can be seen, the only visible organs were the kidneys and the bladder.

CONCLUSION

In this study, the more detailed preclinical aspects of ^{177}Lu-PSMA-617 was presented. The optimized condition for the preparation of this agent was obtained with 15 µg of PSMA, pH of 4-4.5, temperature of 90-95°C. The complex was developed with radiochemical purity of higher than 99% and specific activity of 23.4 MBq/nmol in 35-40 min. The biodistribution of the ^{177}Lu-PSMA-617 complex in different intervals (2-168 h) in numerous organs after intravenous injection into the rats was evaluated. The final results indicated significant accumulation in the kidneys with a fast-temporal decrease. The biodistribution modeling of the complex was done for each organ presenting the cumulative activity of the organs at each time point after injection. The absorbed dose estimation of ^{177}Lu-PSMA-617 showed the highest amount in the kidney with 0.067 mGy/MBq. According to the fast clearance of activity from blood circulation and the kidneys, as the major route of excretion, and besides insignificant activity aggregation in the other organs, this complex can be regarded as an ideal radiolabelled complex for the therapeutic purposes in the patients suffering PCs.

Table 1: The Compartmental Modeling Formulas of Non-Decay Corrected Injected Activity Curves after 177Lu-PSMA-617 Injection to the Syrian Rats

Blood	F1=1.2*exp(-2.64*x)+0.00357* exp (-0.14*x)+0.0768* exp (-0.06*x)+0.0000594* exp (-0.000099*x)
Heart	F2=0.0785385* exp (-0.38*x)+0.0000774* exp (-0.07*x)+0.0010125* exp (-0.00099*x)+0.000441* exp (-0.001*x)+0.01935* exp (-0.077*x)-0.0000041625* exp (-5.14*x)-0.00000000639* exp (-0.24*x)
Lung	F3=0.03* exp (-0.099*x)+0.138736* exp (-0.26*x)+0.0001376* exp (-0.062*x)+0.0024784* exp (-0.001*x)-0.0108* exp (-0.077*x)+0.0012* exp (-0.0523*x)-0.023941546* exp (-0.42*x)-0.00031412* exp (-0.017*x)-0.023141412* exp (-1.18*x)-0.0000258* exp (-0.0999*x)
Stomach	F4=0.6686627* exp (-5.04*x)+8.4899* exp (-0.64*x)+0.039061* exp (-0.14*x)+0.24344* exp (-0.006*x)+0.02544* exp (-0.019*x)-0.282* exp (-0.091*x)
Intestine	F5=0.5* exp (-1.38*x)-0.0018* exp (-0.24*x)-0.0028* exp (-0.24*x)+1.44* exp (-0.57*x)+0.022* exp (-0.0099*x)+0.0196* exp (-0.01*x)+0.0016* exp (-0.077*x)
Liver	F6=0.01791342* exp (-0.45*x)+0.0002408* exp (-0.06*x)+0.0565* exp (-0.0399*x)+0.0001372* exp (-0.001*x)+0.0019* exp (-0.087*x)-0.00001295* exp (-5.04*x)-0.0000000588* exp (-0.14*x)
Spleen	F7=0.1* exp (-0.15*x)-0.185* exp (-3.14*x)-0.0784* exp (-0.03*x)+0.144* exp (-0.67*x)+0.033* exp (-0.0099*x)+0.000196* exp (-1*x)+0.045* exp (-0.0007*x)
Kidney	F8=-0.159* exp (-5.04*x)-0.0000147* exp (-1.64*x)+0.00047* exp (-0.14*x)+2.02* exp (-0.06*x)+0.00000809* exp (-0.000099*x)
Muscle	F9=0.04578723* exp (-0.39*x)+0.0015652* exp (-1.79 *x)+0.0034125* exp (-0.0099*x)+0.008918* exp (-0.031*x)+0.004368* exp (-0.0073*x)-0.00084175* exp (-2.484*x)-0.000012922* exp (-1.674*x)
Pancreas	F10=0.3994026* exp (-0.45*x)+0.00268* exp (-0.077*x)+0.00845* exp (-0.00099*x)+0.00004116* exp (-0.001*x)+0.00007224* exp (-0.06*x)-0.00000005964* exp (-0.14*x)-0.00003885* exp (-5.04*x)
Prostate	F12=17.21026* exp (-1.45*x)+0.00378* exp (-0.077*x)+0.00945* exp (-0.00099*x)+0.0004116* exp (-0.001*x)+0.00007224* exp (-0.06*x)-0.00000005964* exp (-0.14*x)-0.00003885* exp (-5.04*x)
Bone	F11=0.9983* exp (-0.057*x)+0.01* exp (-1.2*x)+0.08956* exp (-0.08*x)+0.002254* exp (-0.0000008*x)+0.021275* exp (-0.38*x)+0.05964* exp (-6.14*x)-0.003266* exp (-0.44*x)

Table 2: Equivalent Absorbed dose Delivered into each Human Organ after Injection of ^{177}Lu-PSMA-617

Target Organ	Equivalent Absorbed dose in Humans (mGy/MBq)	Target Organ	Equivalent Absorbed dose in Humans (mGy/MBq)
Adrenals	0.0005	Muscle	0.0034
Brain	0.0001	Ovaries	0.0003
Breasts	0.0000	Pancreas	0.0042
GB Wall	0.0003	Red Marrow	0.0093
LLI Wall	0.0144	Bone Surf	0.0219
Small Int	0.0003	Spleen	0.0314
Stomach Wall	0.0031	Testes	0.0001
ULI Wall	0.0002	Thymus	0.0002
Heart Wall	0.0023	Thyroid	0.0002
Kidneys	0.0671	UB Wall	0.0002
Liver	0.0031	Total Body	0.0121
Lungs	0.0016		

GW: Gallbladder Wall; LLI: lower large intestine; Int: Intestine; ULI: upper large intestine; UB Wall: Urinary Bladder Wall.
[a] Tissue weighting factors according to international commission on radiological protection, ICRP 103 (2007).

REFERENCES

[1] Ferlay J, Soerjomataram I, Dikshit R, Eser S, Mathers C, Rebelo M, Parkin DM, *et al*. Cancer incidence and mortality worldwide: sources, methods and major patterns in GLOBOCAN 2012. International journal of cancer 2015; 136(5): E359-E86. https://doi.org/10.1002/ijc.29210

[2] Chang SS. Overview of Prostate-Specific Membrane Antigen. Rev Urol 2004; 6(10): 13-18.

[3] Ristau BT, O'Keefe DS, Bacich DJ. The prostate-specific membrane antigen: lessons and current clinical implications

from 20 years of research.Urol Oncol. 2014; 32(3): 272-9. https://doi.org/10.1016/j.urolonc.2013.09.003

[4] Kratochwil C, Giesel FL, Eder M, Afshar-Oromieh A, Benešová M, Mier W, Kopka K, Haberkorn U. [177Lu] Lutetium-labelled PSMA ligand-induced remission in a patient with metastatic prostate cancer. Eur J Nucl Med Mol Imag 2015; 42: 987-8. https://doi.org/10.1007/s00259-014-2978-1

[5] Eder MO, Müller NM, Bauder-Wüst U, Remde Y, Schäfer M, UHennrich M. Novel preclinical and radiopharmaceutical aspects of [68Ga] Ga-PSMA-HBED-CC: a new PET tracer for imaging of prostate cancer. Pharmaceuticals 2014; 7: 779-96. https://doi.org/10.3390/ph7070779

[6] Weineisen M, Simecek J, Schottelius M, Schwaiger M and Wester HJ. Synthesis and preclinical evaluation of DOTAGA-conjugated PSMA ligands for functional imaging and endoradiotherapy of prostate cancer. EJNMMI research 2014; 4: 1-15. https://doi.org/10.1186/s13550-014-0063-1

[7] Kularatne SA, Venkatesh C, Santhapuram HKR, Wang K, Vaitilingam B, Henne WA, Low PS. Synthesis and biological analysis of prostate-specific membrane antigen-targeted anticancer prodrugs. J Med Chem 2010; 53: 7767-77. https://doi.org/10.1021/jm100729b

[8] Malik N, Machulla HJ, Solbach C, Winter G, Reske SN, Zlatopolskiy B. Radiosynthesis of a new PSMA targeting ligand ([18 F] FPy-DUPA-Pep). Applied Radiat Isotopes 2011; 69: 1014-1018. https://doi.org/10.1016/j.apradiso.2011.03.041

[9] Eder M, Schäfer U, Bauder-Wüst S, Hull WE, Wängler C, Mier W, Haberkorn U, Eisenhut M. 68Ga-complex lipophilicity and the targeting property of a urea-based PSMA inhibitor for PET imaging. Bioconjugate Chem 2012; 23: 688-97. https://doi.org/10.1021/bc200279b

[10] Breeman WA, de Blois E, Sze Chan H, Konijnenberg M, Kwekkeboom DJ, Krenning EP. 68Ga-labeled DOTA-peptides and 68Ga-labeled radiopharmaceuticals for positron emission tomography: current status of research, clinical applications, and future perspectives. Semin Nucl Med 2011; 41: 314-21. https://doi.org/10.1053/j.semnuclmed.2011.02.001

[11] Yousefnia H, Amraei N, Hosntalab M, Zolghadri S, Bahrami-Samani A. Preparation and biological evaluation of 166Ho-BPAMD as a potential therapeutic bone-seeking agent. J Radioanal Nucl Chem 2015; 304: 1285-91. https://doi.org/10.1007/s10967-014-3924-1

[12] Sharifi M, Yousefnia H, Zolghadri S, Bahrami-Samani A, Naderi M, Jalilian AR, *et al*. Preparation and biodistribution assessment of 68Ga-DKFZ-PSMA-617 for PET prostate cancer imaging. Nuclear Science and Techniques 2016; 27: 142. https://doi.org/10.1007/s41365-016-0134-2

[13] Zechmann CM, Afshar-Oromieh A, Armor T, Stubbs JB, Mier W, Hadaschik B *et al*. Radiation dosimetry and first therapy results with a 124I/131I-labeled small molecule (MIP-1095) targeting PSMA for prostate cancer therapy. Eur J Nucl Med Mol Imaging 2014; 41: 1280-92. https://doi.org/10.1007/s00259-014-2713-y

[14] Yousefnia H, Radfar E, Jalilian AR, Bahrami-Samani A, Shirvani-Arani S, Arbabi A, Ghannadi-Maragheh M. Development of 177Lu-DOTA-anti-CD20 for radioimmunotherapy. J Radioanal Nucl Chem 2011; 287: 199-209. https://doi.org/10.1007/s10967-010-0676-4

[15] Das T, Guleria MA, Kale C, Shah H, Sarmad HD, Lelec VR, Banerjee S. Clinical translation of 177Lu-labeled PSMA-617: Initial experience in prostate cancer patients. Nucl Med Biol2016; 43: 296-302. https://doi.org/10.1016/j.nucmedbio.2016.02.002

[16] Vaez-Tehrani M, Zolghadri S, Yousefnia H, Afarideh H. Human absorbed dose estimation for a new 175 Yb-phosphonate based on rats data: Comparison with similar bone pain palliation agents. Applied Radiation and Isotopes 2016; 115: 55-60. https://doi.org/10.1016/j.apradiso.2016.06.013

[17] Stabin MG, Siegel JA. Physical models and dose factors for use in internal dose assessment. Health Phys 2003; 85: 294-310 https://doi.org/10.1097/00004032-200309000-00006

[18] Kesner AL, Hsueh WA, Czernin J, Padgett H, Phelps ME, Silverman DH. Radiation dose estimates for [18F] 5-fluorouracil derived from PET-based and tissue-based methods in rats. Mol Imaging Biol 2008; 10: 341-8. https://doi.org/10.1007/s11307-008-0160-5

[19] Yousefnia H, Zolghadri S. Estimated human absorbed dose of a new 153Sm bone seeking agent based on biodistribution data in mice: Comparison with 153Sm-EDTMP. Physica Medica. 2015; 31: 714-9. https://doi.org/10.1016/j.ejmp.2015.05.015

[20] Nair AB, Jacob S. A simple practice guide for dose conversion between animals and human. J Basic Clin Pharm 2016; 7: 27-31. https://doi.org/10.4103/0976-0105.177703

[21] Sparks R, Aydogan B. Comparison of the effectiveness of some common animal data scaling techniques in estimating human radiation dose. Oak Ridge Associated Universities, TN (United States); 1999.

[22] Jacquez JA. Compartmental analysis in biology and medicine: JSTOR; 1985.

[23] Anderson DH. Compartmental modeling and tracer kinetics: Springer Science & Business Media; 2013.

[24] Roberton J. Compartmental distribution of radiotracers. Mayo Clinic, Rochester, MN; 1983.

[25] Bailey DL, Townsend DW, Valk PE, Maisey MN. Positron emission tomography: Springer; 2005. https://doi.org/10.1007/b136169

[26] Wagner JG. Fundamentals of clinical pharmacokinetics. Hamilton, Ill.: Drug Intelligence Publications; 1975.

[27] Yousefnia H, Zolghadri S, Sadeghi HR, Naderi M, Jalilian AR, Shanehsazzadeh S. Preparation and biological assessment of 177Lu-BPAMD as a high potential agent for bone pain palliation therapy: comparison with 177Lu-EDTMP. Journal of Radioanalytical and Nuclear Chemistry 2016; 307: 1243-51. https://doi.org/10.1007/s10967-015-4225-z

[28] Fakhari A, Jalilian AR, Yousefnia H, Shafiee-Ardestani M, Johari-Daha F, *et al*. Development of Radiolanthanide-Labeled-Bis-Alendronate Complexes for Bone Pain Palliation Therapy. Austin J Nucl Med Radiother. 2015; 2: 1012.

[29] AGENCY IAE. Quantifying Uncertainty in Nuclear Analytical Measurements. Vienna: INTERNATIONAL ATOMIC ENERGY AGENCY; 2004.

[30] Yousefnia H, Zolghadri S, Jalilian AR and Naseri Z. Preliminary absorbed dose evaluation of two novel 153Sm bone-seeking agents for radiotherapy of bone metastases: comparison with 153Sm-EDTMP. Journal of Radiotherapy in Practice 2015; 14: 252-9. https://doi.org/10.1017/S1460396915000199

[31] Siegel JA, Thomas SR, Stubbs JB, Stabin MG. MIRD pamphlet no. 16: techniques for quantitative radiopharmaceutical biodistribution data acquisition and analysis for use in human radiation dose estimates. J Nucl Med 1999; 40: 37S-61S.

[32] Lima MF, Pujatti PB, Araújo EB and Mesquita CH.. Compartmental analysis to predict biodistribution in radiopharmaceutical design studies. International nuclear Atlantic conference–INAC 2009.

[33] Bevelacqua J. Internal dosimetry primer. Radiation protection management 2005; 22: 7.

[34] Stabin MG, Sparks RB, Crowe E. OLINDA/EXM: the second-generation personal computer software for internal dose assessment in nuclear medicine. J Nucl Med 2005; 46: 1023-7.

[35] KhalidM, BokhariTH, AhmadM, BhattiHN, Iqbal M, *et al*. Evaluation of Carrier added and no Carrier added 90Y-EDTMP as Bone Seeking therapeutic radiopharmaceutical. Pak J Pharm Sci 2014; 27: 813-8.

[36] Afshar-Oromieh A, Malcher A, Eder M, Eisenhut M, Linhart H, Hadaschik B *et al*. PET imaging with a [68Ga] gallium-labelled PSMA ligand for the diagnosis of prostate cancer: biodistribution in humans and first evaluation of tumour lesions. Eur J Nucl Med Mol Imaging 2013; 40: 486-95. https://doi.org/10.1007/s00259-012-2298-2

Received on 15-10-2017 Accepted on 21-11-2017 Published on 04-12-2017

http://dx.doi.org/10.15379/2408-9788.2017.04.02.01